ELSEVIER

www.elsevier.nl/locate/jorganchem

Journal of Organometallic Chemistry 596 (2000) 136–143

Journal of Organometallic Chemistry

Synthesis, characterization, and X-ray crystallography of a series of ditungsten complexes with bis(diphenylphosphino)amine

Judith L. Eglin [a,*], Laura T. Smith [a], Richard J. Staples [b], Edward J. Valente [c], Jeffrey D. Zubkowski [d]

[a] *Department of Chemistry at Mississippi State University, Mississippi State, MS 39762, USA*
[b] *Department of Chemistry, Harvard University, Cambridge, MA 02138, USA*
[c] *Department of Chemistry at Mississippi College, Clinton, MS 39058, USA*
[d] *Department of Chemistry at Jackson State University, Jackson, MS 39217, USA*

Received 2 August 1999

Dedicated to Professor F.A. Cotton on the occasion of his 70th birthday.

Abstract

The W_2(II, II) and W_2(III, III) compounds, $W_2(\mu\text{-}O_2CC_6H_5)_2Cl_2(\mu\text{-dppa})_2$ (**1**), $W_2(\mu\text{-}O_2CC_6H_5)_2Br_2(\mu\text{-dppa})_2$ (**2**), $W_2(\mu\text{-}O_2CC_6H_5)_2I_2(\mu\text{-dppa})_2$ (**3**), $W_2Cl_4(\mu\text{-dppa})_2$ (**4**), $W_2(\mu\text{-Cl})_2Cl_4(\mu\text{-dppa})_2$ (**5**), and $W_2(\mu\text{-H})_2Cl_4(\mu\text{-dppa})_2$ (**6**), have been synthesized using the chelating phosphine ligand dppa (bis(diphenylphosphino)amine). The series of metal–metal multiply bonded complexes has been characterized by NMR and UV–vis spectroscopy, and the structures of **2**·$(THF)_2$, **5**·$(THF)_4$, and **6**·$(THF)_2$ determined by X-ray crystallography.

Keywords: Ditungsten; Metal–metal multiple bond; Phosphine

1. Introduction

The compounds $W_2(\mu\text{-}O_2CC_6H_5)_2Cl_2(\mu\text{-dppa})_2$ (**1**), $W_2(\mu\text{-}O_2CC_6H_5)_2Br_2(\mu\text{-dppa})_2$ (**2**), $W_2(\mu\text{-}O_2CC_6H_5)_2I_2(\mu\text{-dppa})_2$ (**3**), $W_2Cl_4(\mu\text{-dppa})_2$ (**4**), $W_2(\mu\text{-Cl})_2Cl_4(\mu\text{-dppa})_2$ (**5**), and $W_2(\mu\text{-H})_2Cl_4(\mu\text{-dppa})_2$ (**6**) have been synthesized using a simpler synthetic route to multiply bonded ditungsten complexes with the ability to easily vary the coordinated ligands of W_2(II, II) and related compounds [1–6]. Previously, the potential of $W_2(\mu\text{-}O_2CC_6H_5)_4$ [7] as a starting material concentrated on the use of the phosphine ligand dppm (bis(diphenylphosphino)methane) with ZnX_2 as the halide source to synthesize quadruply bonded complexes of the general type $W_2(\mu\text{-}O_2CC_6H_5)_2X_2(\mu\text{-dppm})_2$ where X is Cl, Br and I; the axially coordinated halide [4]. The extension of this project to the chelating phosphine dppa (bis(diphenylphosphino)amine) resulted in the synthesis and spectroscopic characterization of a series of $W_2(\mu\text{-}O_2CC_6H_5)_2X_2(\mu\text{-dppa})_2$ complexes as well as the related W_2(II, II) compound $W_2Cl_4(dppa)_2$ and two edge-sharing bioctahedral (ESBO) W_2(III, III) complexes, $W_2(\mu\text{-Cl})_2Cl_4(\mu\text{-dppa})_2$ and $W_2(\mu\text{-H})_2Cl_4(\mu\text{-dppa})_2$ [6,8–11]

2. Results and discussion

2.1. Preparation and general properties

Investigations in our laboratory have shown that the quadruply bonded material $W_2(\mu\text{-}O_2CC_6H_5)_4$ [7] provides a relatively stable, easily synthesized dinuclear starting material for compounds of the general type $W_2(\mu\text{-}O_2CC_6H_5)_2X_2(dppm)_2$ where X is Cl, Br, and I [4]. The original study of the reactivity of $W_2(\mu\text{-}O_2CC_6H_5)_4$ [7] with ZnX_2 and dppm [4] has been extended to the chelating phosphine dppa with the synthesis of the $W_2(\mu\text{-}O_2CC_6H_5)_2X_2(\mu\text{-dppa})_2$ series of complexes with X = Cl, Br, and I.

In addition to the synthesis of the series of $W_2(\mu\text{-}O_2CC_6H_5)_2X_2(dppa)_2$ compounds, the related com-

* Corresponding author.

0022-328X/00/$ - see front matter
PII: S0022-328X(99)00610-5

pounds $W_2Cl_4(\mu\text{-dppa})_2$, $W_2(\mu\text{-Cl})_2Cl_4(\mu\text{-dppa})_2$, and $W_2(\mu\text{-H})_2Cl_4(\mu\text{-dppa})_2$ have been prepared from WCl_4 and dppa using $NaBEt_3H$ as the reducing agent [4,12,13]. $W_2(\mu\text{-H})_2Cl_4(\mu\text{-dppa})_2$ is the third W_2(III, III) dihydride species synthesized in our laboratory. Other compounds in the series are $W_2(\mu\text{-H})_2(\mu\text{-}O_2CC_6H_5)_2Cl_2(P(C_6H_5)_3)_2$ [6] and $W_2(\mu\text{-H})_2Cl_4(\mu\text{-dppm})_2$ [11]. Unlike the synthesis of $W_2(\mu\text{-H})_2Cl_4(\mu\text{-dppm})_2$ that requires heating of $W_2Cl_4(\mu\text{-dppm})_2$ in the presence of H_2 [11], the formation of $W_2(\mu\text{-H})_2Cl_4(\mu\text{-dppa})_2$ occurs at room temperature from the oxidative addition of H_2 to $W_2Cl_4(\mu\text{-dppa})_2$. The related ESBO compound $W_2(\mu\text{-Cl})_2Cl_4(\mu\text{-dppa})_2$ results from a one-electron reduction of WCl_4 in the presence of dppa [3,14–17].

2.2. Structures

The coordination geometry about the quadruply bonded ditungsten core ($\sigma^2\pi^4\delta^2$) in both the dppm and dppa series of $W_2(\mu\text{-}O_2CC_6H_5)_2X_2(\mu\text{-P-P})_2$ complexes remains eclipsed without weakening of the δ bond due to incomplete overlap [18]. However, MO calculations performed on the model compound $W_2(\mu\text{-}O_2CH)_2I_2(PH_3)_4$ demonstrate that the axial ligands effectively reduce the strength of the W–W σ bond [4]. Compared to the W–W bond distance of $W_2Br_4(\mu\text{-dppm})_2$ (2.2632(9) Å), a slight increase in the metal–metal bond distance is observed for $W_2(\mu\text{-}O_2CC_6H_5)_2Br_2(\mu\text{-dppa})_2$ [7]. A similar trend is observed for the dimolybdenum series of $Mo_2X_4(\mu\text{-dppa})_2$ and $Mo_2(\mu\text{-}O_2CCH_3)_2X_2(\mu\text{-dppa})_2$ complexes where X is Cl and Br [19]. However, the W–W bond distance of **2**·$(THF)_2$ (2.2986(11) Å) and the related compound $W_2(\mu\text{-}O_2CC_6H_5)_2I_2(\mu\text{-dppm})_2$ (2.2925(6) Å) [4] are essentially the same, with no significant variation due to a change in the chelating phosphine ligand. Of note in the structure of **2**·$(THF)_2$ is the presence of hydrogen bonding between interstitial solvent and the amine protons of the dppa ligands (Fig. 1). The oxygen atoms of the THF solvent molecules are 1.957 Å from the protons of the bridging N–*H* atoms in the dppa ligands.

As expected [4], the W–Br bond distance of the axially coordinated bromide in **2**·$(THF)_2$ is longer (2.857(2) Å) than observed for the equatorial W–Br bond distances in $W_2Br_4(\mu\text{-dppm})_2$ of 2.507(3) and 2.520(3) Å [12]. The difference in the distances of the W–I bond distance of $W_2(\mu\text{-}O_2CC_6H_5)_2I_2(\mu\text{-dppm})_2$ (3.1033(7) Å) and the W–Br bond distance of **2**·$(THF)_2$ reflects the change in ionic radius, I versus Br. The W–W–Br bond angle of **2**·$(THF)_2$ is 171.97(4)° and further studies of the $W_2(\mu\text{-}O_2CC_6H_5)_2X_2(\mu\text{-P-P})_2$ series of complexes will focus on the substitution of the axial halides.

The bond distances and angles of $W_2(\mu\text{-Cl})_2Cl_4(\mu\text{-dppa})_2\cdot(THF)_4$ vary minimally from the bond distances and angles observed in $W_2(\mu\text{-Cl})_2Cl_4(\mu\text{-dppm})_2$ with a

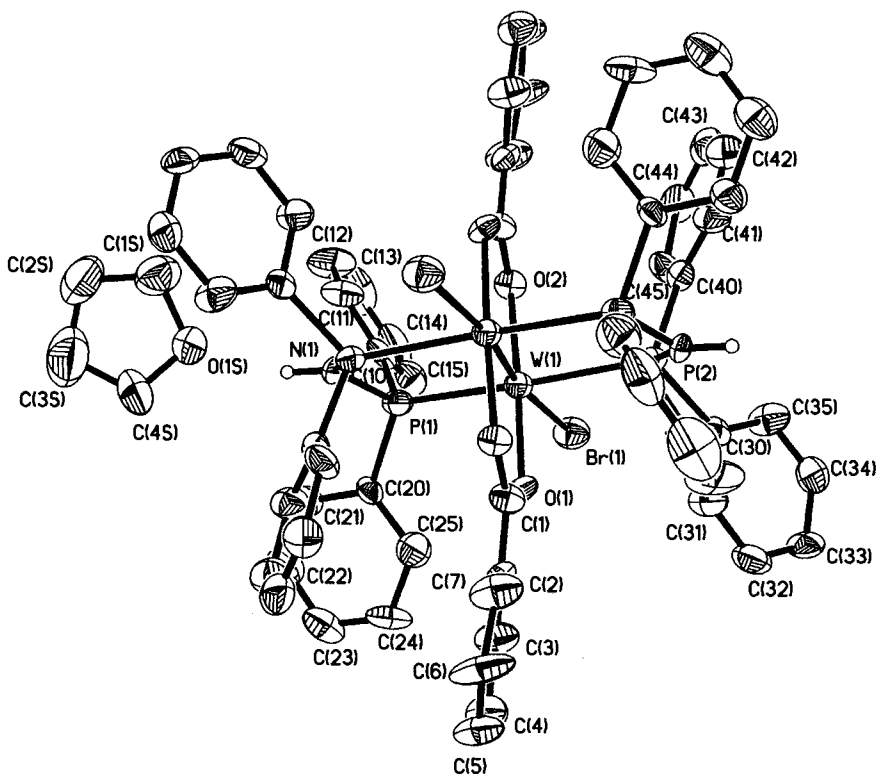

Fig. 1. ORTEP drawing of $W_2(\mu\text{-}O_2CC_6H_5)_2Br_2(\mu\text{-dppa})_2\cdot(THF)_2$ (**2**·$(THF)_2$). The thermal ellipsoids are drawn at 50% probability. With the exception of the N–*H* atoms, hydrogen atoms have been omitted for clarity.

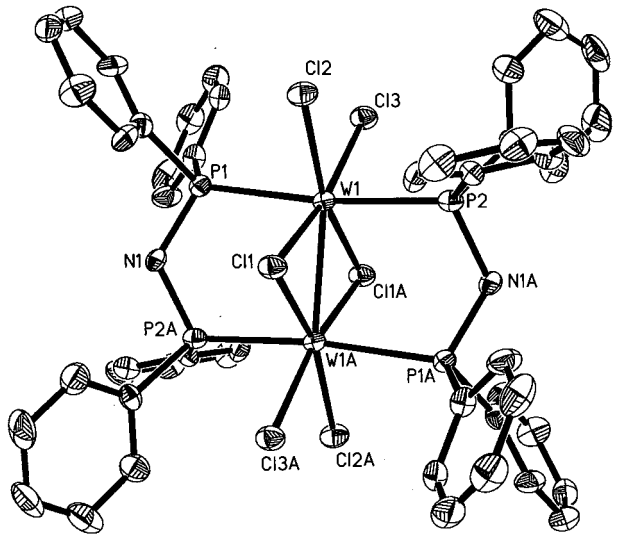

Fig. 2. ORTEP drawing of $W_2(\mu\text{-}Cl)_2Cl_4(\mu\text{-}dppa)_2\cdot(THF)_4$ (**5**·$(THF)_4$). The thermal ellipsoids are drawn at 50% probability. Hydrogen atoms have been omitted for clarity.

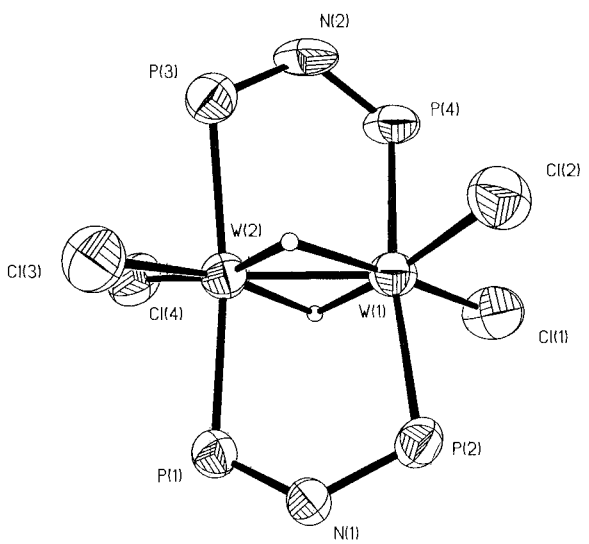

Fig. 3. ORTEP drawing of the $W_2(\mu\text{-}H)_2Cl_4P_4$ core of $W_2(\mu\text{-}H)_2Cl_4(\mu\text{-}dppa)_2\cdot(THF)_2$ (**6**·$(THF)_2$). The thermal ellipsoids are drawn at 50% probability.

W–W bond distance of 2.691(1) Å, W–Cl_b bond distances of 2.405(3) and 2.393(3) Å, a W–Cl_b–W bond angle of 68.23(9)°, and a W–W–Cl_t bond angle of 137.65° [20]. Unlike the structure of **2**·$(THF)_2$, the closest oxygen atom of the THF solvent molecule is 3.105 Å from the proton of the bridging amine of the dppa ligand.

The W–W bond distance of the W_2(III, III) ESBO complex $W_2(\mu\text{-}H)_2Cl_4(\mu\text{-}dppa)_2\cdot(THF)_2$ (2.407(2) Å) is only 0.1 Å longer than the quadruply bonded compound $W_2(\mu\text{-}O_2CC_6H_5)_2Br_2(\mu\text{-}dppa)_2\cdot(THF)_2$ and over 0.2 Å shorter than $W_2(\mu\text{-}Cl)_2Cl_4(\mu\text{-}dppa)_2\cdot(THF)_4$. With W–W bond distances of 2.3918(7) Å for $W_2(\mu\text{-}H)_2Cl_4(\mu\text{-}dppm)_2$ [11] and 2.3500(12) Å for $W_2(\mu\text{-}H)_2Cl_2(PPh_3)_2(\mu\text{-}O_2CC_6H_5)_2$ [6], $W_2(\mu\text{-}H)_2Cl_4(\mu\text{-}dppa)_2\cdot(THF)_2$ contains the longest W–W bond distance observed to date for a W_2(III, III) ESBO dihydride compound. As a result of the increase in the metal–metal bond distance of **6**·$(THF)_2$, the W–H bond distances are longer (2.025(20) and 2.134(20) Å) than the W–H bond distances observed previously in either $W_2(\mu\text{-}H)_2Cl_4(\mu\text{-}dppm)_2$ (1.83(8) and 1.74(8) Å) [11] or $W_2(\mu\text{-}H)_2Cl_2(PPh_3)_2(\mu\text{-}O_2CC_6H_5)_2$ (1.67(8) and 1.90(8) Å) [6] (Figs. 2 and 3). Analogous to the structure of **2**·$(THF)_2$, the protons of the N–*H* in the dppa ligands are hydrogen bonded (1.986 and 2.208 Å) to THF solvent molecules.

2.3. NMR spectroscopy

The ^{31}P-NMR spectrum for $W_2(\mu\text{-}O_2CC_6H_5)_2Br_2(\mu\text{-}dppa)_2$ (**2**) contains a singlet at 92.88 ppm with J_{W-P} coupling of 108 and 290 Hz. The ^{31}P-NMR spectra of **1** and **3** are similar to that of **2** with singlets at 92.88 ppm (J_{W-P} coupling of 116 and 288 Hz) and 92.91 ppm (J_{W-P} coupling of 113 and 297 Hz) respectively and confirm the general structures of **1** and **3**. Slight increases in the chemical shift on progression through the series from Cl to I are observed for both the dppa ligand series **1**–**3** and the $W_2(\mu\text{-}O_2CC_6H_5)_2X_2(\mu\text{-}dppm)_2$ series [4]. A large ^{31}P chemical shift difference of approximately 47 ppm is observed between **1**–**3** and the free phosphine ligand. A smaller ^{31}P chemical shift difference (Δ 23 ppm) is observed in comparison of **1**–**3** to $W_2Cl_4(\mu\text{-}dppa)_2$, as observed for the analogous series with dppm [4].

The related dimolybdenum compounds, $Mo_2(\mu\text{-}O_2CCH_3)_2X_2(\mu\text{-}dppa)_2$, have chemical shifts of 78.7 (Cl), 77.8 (Br), 75.2 (I), and 80.4 ppm (acetonitrile) with the larger shift of the acetonitrile compound attributed to the ionic character of the molecule [21,22]. A change in the phosphine ligand in the dimolybdenum studies from the dppa to the dppma (bis(diphenylphosphino)methylamine) ligand results in chemical shift differences of 27 ppm from the free phosphine ligand for $Mo_2(\mu\text{-}O_2CCH_3)_2X_2(\mu\text{-}dppma)_2$ in contrast to 36 ppm observed for $Mo_2X_2(\mu\text{-}O_2CCH_3)_2(\mu\text{-}dppa)_2$ [23]. The extreme sensitivity of the phosphorus chemical shift to the nature of the bridging phosphine and carboxylate ligands is demonstrated by the changes in chemical shift upon a change in the bridging ligand for both the ditungsten and dimolybdenum compounds [4,19,21–23].

The ^{31}P-NMR spectrum of $W_2Cl_4(\mu\text{-}dppa)_2$ contains a singlet at 69.9 ppm with J_{W-P} coupling of 138 Hz. The ^{31}P-NMR spectrum of $W_2(\mu\text{-}H)_2Cl_4(\mu\text{-}dppa)_2$ contains a singlet at 73.8 ppm and J_{W-P} coupling of 145 Hz. The ^{31}P-NMR chemical shifts of **4** and **6** are quite similar with a difference of only 3.9 ppm, slightly larger

than the chemical shift difference observed for $W_2Cl_4(\mu\text{-dppm})_2$ and $W_2(\mu\text{-H})_2Cl_4(\mu\text{-dppm})_2$ (Δ 2.3 ppm) [4,11]. ^{31}P-NMR spectra of the reaction mixture of $W_2Cl_4(\mu\text{-dppa})_2$ obtained at intervals over several hours indicate the formation of $W_2(\mu\text{-H})_2Cl_4(\mu\text{-dppa})_2$ at room temperature. The ^{1}H-NMR spectrum of $W_2(\mu\text{-H})_2Cl_4(\mu\text{-dppa})_2$ confirmed the presence of the bridging hydrides with a pentet observed at a chemical shift of 5.514 ppm with J_{H-P} coupling of 6.4 Hz and J_{H-W} coupling of 109 Hz.

Based on Fenske–Hall calculations in the model compound $W_2(\mu\text{-H})_2(\mu\text{-}O_2CH)_2(PH_3)_2Cl_2$, a W–W triple bond is predicted ($\sigma^2\pi^2\delta^2$) with a large HOMO–LUMO gap ($\sim$2.7 eV) [6]. The temperature independence of the ^{31}P-NMR spectra of $W_2(\mu\text{-H})_2Cl_4(\mu\text{-dppm})_2$ and the narrow linewidths of both the $W_2(\mu\text{-H})_2Cl_4(\mu\text{-dppm})_2$ and $W_2(\mu\text{-H})_2Cl_4(\mu\text{-dppa})_2$ spectra confirm the presence of a large HOMO–LUMO gap and the diamagnetism of compounds of this type [11]. In contrast, magnetic studies of $W_2(\mu\text{-Cl})_2Cl_4(\mu\text{-dppm})_2$ reflect the partial occupancy of the δ^* orbital at r.t., and a magnetic moment of 0.70 B.M. is observed at 24°C [14,24]. The ^{31}P-NMR spectrum of $W_2(\mu\text{-Cl})_2Cl_4(\mu\text{-dppa})_2$ obtained at 23.5°C contained a broad singlet, $\Delta\nu_{1/2} = 329$ Hz, at -23.5 ppm.

2.4. UV–vis spectroscopy

Unlike the $W_2(\mu\text{-}O_2CC_6H_5)_2X_2(\mu\text{-dppm})_2$ series with δ to δ^* transitions at 454 nm for X = Cl, 438 nm for X = Br, and 400 nm for X = I [4], the $W_2(\mu\text{-}O_2CC_6H_5)_2X_2(\mu\text{-dppa})_2$ series does not vary systematically with a change in halide. In the case of $W_2(\mu\text{-}O_2CC_6H_5)_4$, the presence of axial ligands in the solutions for UV–vis spectroscopy resulted in absorption bands at shorter wavelengths by 30 nm as a result of weakening of the W–W bond strength [7]. Without additional structural information for the $W_2(\mu\text{-}O_2CC_6H_5)_2X_2(\mu\text{-dppa})_2$ series, the basis [4,25–28] for the changes in the UV–vis spectra across the series [436 nm for X = Cl, 382 nm for X = Br, and 442 nm for X = I] cannot be determined.

Analogous to the electronic spectra of other W_2(III, III) ESBO complexes, both the ligand-to-metal charge transfer band (381 nm) and the prominent absorption band between 450 and 550 nm (469 nm) are observed in the UV–vis spectrum of $W_2(\mu\text{-Cl})_2Cl_4(\mu\text{-dppa})_2$ [29].

3. Experimental

3.1. General procedures

Standard Schlenk, vacuum line, and drybox techniques were used with an argon atmosphere. Commercial grade THF, toluene, and hexanes were dried over potassium–sodium benzophenone ketyl and methylene chloride was dried over P_2O_5. All solvents were freshly distilled under an atmosphere of argon prior to use. The starting material WCl_4 was synthesized from WCl_6 and $W(CO)_6$ using the previously reported method [30]. The chelating phosphine ligand dppa was purchased from Strem Chemicals and kept under dynamic vacuum overnight to remove any residual oxygen or moisture. Tri-*n*-butyl phosphine was purchased from Johnson Matthey, used without further purification, and transferred under an atmosphere of argon. $NaO_2CC_6H_5$ was obtained from Matheson Coleman and Bell, and all residual oxygen and moisture was removed by heating the salt to 200° C for 6 h under dynamic vacuum. $NaBEt_3H$ was purchased as a 1 M solution in toluene from Aldrich Chemical Company and used without further purification. $ZnCl_2$, $ZnBr_2$, and ZnI_2 were purchased from Aldrich Chemical Company and all transfers performed under an argon atmosphere.

$^{31}P\{^1H\}$-NMR spectra (162 MHz) were recorded on a General Electric instrument using an Omega NMR spectrometer with a 10 mm broad band probe and referenced externally to H_3PO_4 (0.0 ppm). ^{1}H-NMR spectra (400 MHz) were recorded on the same spectrometer with a 5 mm probe and referenced to TMS. The UV–vis spectra were recorded on a Hewlett–Packard 8452 model diode array spectrophotometer from 190 to 820 nm. Magnetic susceptibility measurements were performed on a Johnson Matthey Magnetic Susceptibility Balance and diamagnetic corrections were applied [31].

3.2. Preparation of $W_2(\mu\text{-}O_2CC_6H_5)_2Cl_2(\mu\text{-dppa})_2$ (1)

A gray mixture of WCl_4 (0.500g, 1.54 mmol) and $NaO_2CC_6H_5$ (0.443 g, 3.07 mmol) was dissolved in 10 ml of THF and cooled to $-70°$ C in an ethanol–dry ice bath. After slow addition of 3.07 ml (3.07 mmol) of $NaBEt_3H$, the reaction was allowed to warm until the color of the solution changed from the initial gray to a brilliant purple. A THF (5 ml) solution of dppa (0.592 g, 1.54 mmol) and $ZnCl_2$ (0.320 g, 2.35 mmol) was transferred by cannula to the purple solution, and the ethanol–dry ice bath was removed. The solution turned a brick-red color within 30 min of warming to room temperature (r.t.), and the complex was precipitated with the addition of 30 ml of hexanes. After washing the reaction mixture three times with 30 ml aliquots of hexanes, the remaining solvent was removed under dynamic vacuum. The solid was dissolved in THF, filtered through Celite, and dried under dynamic vacuum to yield 1.57 g (70.4%) of a brick-red product. Visible spectrum (THF, λ_{max}, nm): 436 sh.

3.3. Preparation of $W_2(\mu\text{-}O_2CC_6H_5)_2Br_2(\mu\text{-dppa})_2$ (2)

The bromide analog was obtained by the same methodology used to synthesize $W_2(\mu\text{-}O_2CC_6H_5)_2Cl_2(\mu\text{-dppa})_2$. $ZnBr_2$ (0.346 g, 2.16 mmol) instead of $ZnCl_2$ was used to yield $W_2(\mu\text{-}O_2CC_6H_5)_2Br_2(\mu\text{-dppa})_2$ (1.319 g, 55.8%). The amounts of starting material WCl_4 and the other reagents used were the same. Visible spectrum (THF, λ_{max}, nm): 382 sh.

3.4. Preparation of $W_2(\mu\text{-}O_2CC_6H_5)_2I_2(\mu\text{-dppa})_2$ (3)

$W_2(\mu\text{-}O_2CC_6H_5)_2I_2(\mu\text{-dppa})_2$ was obtained by the same methodology used to synthesize the other halide analogs **1** and **2**. The same amounts of starting material WCl_4 and the other reagents were used with the halide source ZnI_2 (0.490 g, 1.54 mmol) to yield $W_2(\mu\text{-}O_2CC_6H_5)_2I_2(\mu\text{-dppa})_2$ (1.53 g, 61.3%). Visible spectrum (THF, λ_{max}, nm): 442 sh.

3.5. Preparation of $W_2Cl_4(\mu\text{-dppa})_2$ (4)

The gray powder WCl_4 (0.500 g, 1.54 mmol) was suspended in 10 ml of THF and cooled to −60°C in an ethanol–dry ice bath. To this suspension, 3.07 ml (3.07 mmol) of $NaBEt_3H$ was added and the mixture warmed to −20°C. The 'WCl_2' solution was then transferred by cannula to a flask at r.t. containing 0.60 g (1.6 mmol) of dppa. The reaction mixture was warmed to r.t. with copious amounts of brown powder and a brown supernatant appearing in the solution. After washing the reaction mixture three times with 30 ml aliquots of hexanes, all solvent was removed under dynamic vacuum to yield 0.800 g (81.4%) of the brown product. If reaction times are increased, the formation of $W_2(\mu\text{-}H)_2Cl_4(\mu\text{-dppa})_2$ occurs within several hours after the addition of dppa. Visible spectrum (THF, λ_{max}, nm): 454.

3.6. Preparation of $W_2(\mu\text{-}Cl)_2Cl_4(\mu\text{-dppa})_2$ (5)

WCl_4 (1.00 g, 3.08 mmol) was suspended in 10 ml of THF and cooled to −60°C in an ethanol–dry ice bath. To this mixture, 3.07 ml (3.07 mmol) of $NaBEt_3H$ was added and the solution warmed to −20°C. The 'WCl_2' solution was then transferred by cannula to a flask at r.t. containing 1.20 g (3.20 mmol) of dppa. The reaction mixture was warmed to r.t., stirred overnight, and washed three times with 30 ml aliquots of hexanes to yield an orange–red powder. Upon solvent removal under dynamic vacuum, 1.87 g (74.1%) of orange-red powder (**5**) was produced. Visible spectrum (THF, λ_{max}, nm): 381, 469; ^{1}H-NMR spectrum (CD_2Cl_2, ppm): 7.63 (s), 7.54 (s), 7.43 (s) with 1:2:2 integrated ratio.

3.7. Preparation of $W_2(\mu\text{-}H)_2Cl_4(\mu\text{-dppa})_2$ (6)

WCl_4 (1.0 g, 3.07 mmol) was suspended in 10 ml of THF. After the flask was cooled to −60°C in an ethanol–dry ice bath, 6.14 ml of $NaBEt_3H$ (6.14 mmol) was added. The reaction was allowed to warm to −20°C and a green solution formed. Tri-*n*-butyl phosphine (1.52 ml, 6.14 mmol) was added, and the solution allowed to warm to r.t. A THF (10 ml) solution of dppa (1.18 g, 3.07 mmol) was transferred by cannula to the green product $W_2Cl_4(P(n\text{-}Bu)_3)_4$, and the reaction mixture heated gently for 48 h to yield a deep purple solid product upon addition of hexanes. The precipitate was washed several times with 30 ml aliquots of hexanes and solvent removed under dynamic vacuum to yield 0.843 g (42.8%) of the purple product. Visible spectrum (CH_2Cl_2, λ_{max}, nm): 378, 548, 752; ^{1}H-NMR spectrum ($CDCl_3$, ppm): 7.99 (m), 7.138 (m) with 2:3 integrated ratio, 5.514 ppm (pentet).

3.8. Crystallographic studies

Crystals of $W_2(\mu\text{-}O_2CC_6H_5)_2Br_2(\mu\text{-dppa})_2\cdot(THF)_2$ (**2**·$(THF)_2$), $W_2(\mu\text{-}Cl)_2Cl_4(\mu\text{-dppa})_2\cdot(THF)_4$ (**5**·$(THF)_4$) and $W_2(\mu\text{-}H)_2Cl_4(\mu\text{-dppa})_2\cdot(THF)_2$ (**6**·$(THF)_2$) were grown from THF–hexanes solvent mixtures. Data were collected for **2**·$(THF)_2$ and **5**·$(THF)_4$ using a Siemens SMART CCD-based diffractometer equipped with a LT-2 low-temperature apparatus operating at 213 K. A suitable crystal was mounted on a glass fiber using grease. Data were measured using omega scans of 0.3° per frame for 30 s, such that a hemisphere was collected. A total of 1271 frames was collected with a final resolution of 0.80 Å for **2**·$(THF)_2$ and 0.75 Å for **5**·$(THF)_4$. The first 50 frames were recollected at the end of each data collection to monitor for decay, but neither of the crystals used for the diffraction study showed decomposition during data collection. Cell parameters were retrieved using SMART [32] software and refined using SAINT on all observed reflections. Data reduction was performed using the SAINT software [33], which corrects for decay and Lorentz and polarization effects. Absorption corrections were applied using SADABS [34] supplied by George Sheldrick. The structure was solved by direct methods using the SHELXL-90 [35] program and refined by least squares method on F^2, SHELXL-93 [36], incorporated in SHELXTL 5.03 (PC-Version) [37].

The structures of **2**·$(THF)_2$ and **5**·$(THF)_4$ were solved in the space groups $P2_1/n$ and $P\bar{1}$, respectively, by analysis of systematic absences. All non-hydrogen atoms were refined anisotropically. The hydrogen atoms were calculated by geometrical methods and refined as a riding model. The crystal quality yielded poor data beyond 0.9 Å for **2**·$(THF)_2$ and this data was not used in the refinement. Pertinent crystallographic

Table 1
Crystal data for compounds **2**·$(THF)_2$, **5**·$(THF)_4$, and **6**·$(THF)_2$

	$W_2(\mu\text{-}O_2CC_6H_5)_2Br_2(\mu\text{-dppa})_2\cdot(THF)_2$ (**2**·$(THF)_2$)	$W_2(\mu\text{-}Cl)_2Cl_4(\mu\text{-dppa})_2\cdot(THF)_4$ (**5**·$(THF)_4$)	$W_2(\mu\text{-}H)_2Cl_4(\mu\text{-dppa})_2\cdot(THF)_2$ (**6**·$(THF)_2$)
Formula	$C_{70}H_{68}Br_2N_2O_6P_4W_2$	$C_{64}H_{74}Cl_6N_2P_4W_2$	$C_{56}H_{60}Cl_4N_2P_4W_2$
Formula weight	1684.66	1639.53	1426.44
Temperature (K)	213(2)	213(2)	294(2)
Wavelength (Å)	0.71073	0.71073	0.71073
Crystal system	Monoclinic	Triclinic	Monoclinic
Space group	$P2_1/n$, [no. 14]	$P\bar{1}$ [no. 2]	$P2_1/c$ [no. 14]
a (Å)	11.382(2)	10.4264(2)	22.43(2)
b (Å)	20.453(7)	12.1319(2)	15.34(2)
c (Å)	13.871(4)	13.9311(2)	17.794(10)
α (°)		67.339(1)	
β (°)	97.86(2)	78.524(1)	109.71(5)
γ (°)		85.979(1)	
V (Å^3)	3199(2)	1593.58(5)	5763(8)
Z	2	1	4
D_{calc} (Mg m^{-3})	1.749	1.708	1.644
Absorption coefficient (mm^{-1})	4.997	4.007	4.415
Data/restraints/parameters	4137/0/388	4113/60/370	7618/0/632
R_1	0.0554 [a]	0.0414 [a]	0.0413 [a]
wR_2	0.1009 [b]	0.0875 [b]	0.0688 [b]

[a] $R_1 = \Sigma||F_o|-|F_c||/\Sigma|F_o|$.
[b] $wR_2 = [\Sigma(wF_o^2-F_c^2)^2/\Sigma(wF_o^4)]^{1/2}$.

parameters for **2**·$(THF)_2$ and **5**·$(THF)_4$ are summarized in Table 1. Selected bond lengths and angles for **2**·$(THF)_2$ and **5**·$(THF)_4$ are listed in Tables 2 and 3.

Data for $W_2(\mu\text{-}H)_2Cl_4(\mu\text{-dppa})_2\cdot(THF)_2$ (**6**·$(THF)_2$) were collected on a Siemens R3m/V automated diffractometer fitted with a molybdenum source and a graphite monochrometer [38]. The crystal was mounted in a 0.2 mm glass capillary and the cell determined by careful alignment of 32 high-order diffraction intensities. Since no decomposition was observed over the course of data collection, the data were corrected for Lorentz and polarization effects, but not for decomposition or absorption.

Application of the Patterson function located the two tungsten atoms and successive difference Fourier maps revealed the remaining non-hydrogen atoms [39,40]. In the final model, all non-hydrogen atoms positions and attendant anisotropic displacement factors were refined with hydrogen atoms in calculated positions with isotropic vibrational factors 20% greater than the attached atom contributing to the calculated structure factors. The bridging hydrides were located between the tungsten atoms upon inspection of the final difference Fourier map. A fixed isotropic vibrational amplitude of 0.0552 was assigned to each hydride to yield stable refinement of the positional coordinates with other difference features remaining in the range 1–2 e^{-3}. Phenyl carbons C43 through C48 have considerably broadened anisotropic displacement factors that appear to be due to a dynamic in-plane vibration of the ring. Attempts to model the region as a static disorder of two contributing locations were unsuccessful. A small extinction parameter was applied and refinement was performed against F^2. Scattering factors were taken

Table 2
Selected bond lengths (Å) and angles (°) for **2**·$(THF)_2$

Bond lengths	
W(1)–W(1A)	2.2986(11)
W(1)–P(1)	2.541(3)
W(1)–P(2)	2.517(3)
W(1)–O(1)	2.096(7)
W(1)–O(2)	2.078(7)
W(1)–Br(1)	2.857(2)
Bond angles	
O(1)–W(1)–W(1A)	88.4(2)
O(2)–W(1)–W(1A)	89.9(2)
O(2)–W(1)–O(1)	177.4(3)
O(1)–W(1)–P(1)	95.6(2)
O(2)–W(1)–P(1)	82.8(2)
O(1)–W(1)–P(2)	93.5(2)
O(2)–W(1)–P(2)	88.5(2)
W(1A)–W(1)–P(1)	102.82(8)
W(1A)–W(1)–P(2)	90.28(8)
P(2)–W(1)–P(1)	164.21(11)
O(1)–W(1)–Br(1)	94.9(2)
O(2)–W(1)–Br(1)	87.0(2)
W(1A)–W(1)–Br(1)	171.97(4)
P(1)–W(1)–Br(1)	84.13(8)
P(2)–W(1)–Br(1)	82.26(9)

Table 3
Selected bond lengths (Å) and angles (°) for compound **5**·$(THF)_4$

Bond lengths	
W(1)–W(1A)	2.6828(8)
W(1)–Cl(1)	2.394(2)
W(1)–Cl(2)	2.421(2)
W(1)–Cl(3)	2.422(2)
W(1)–P(1)	2.582(2)
W(1)–P(2)	2.541(3)
Bond angles	
Cl(1A)–W(1)–Cl(1)	111.76(6)
W(1A)–Cl(1)–W(1)	68.24(6)
Cl(2)–W(1)–W(1A)	139.41(6)
Cl(3)–W(1)–W(1A)	136.66(6)
Cl(2)–W(1)–Cl(3)	83.86(8)
Cl(2)–W(1)–P(1)	87.73(8)
Cl(3)–W(1)–P(1)	89.81(8)
Cl(2)–W(1)–P(2)	85.23(8)
Cl(3)–W(1)–P(2)	88.07(8)
P(1)–W(1)–W(1A)	93.51(6)
P(2)–W(1)–W(1A)	92.75(6)
P(2)–W(1)–P(1)	172.82(8)

from the International Tables for X-Ray Crystallography [41]. Crystallographic parameters for **6**·$(THF)_2$ are summarized in Table 1 with selected bond lengths and angles for **6**·$(THF)_2$ listed in Table 4.

Table 4
Selected bond lengths (Å) and angles (°) compound **6**·$(THF)_2$

Bond lengths			
W(1)–W(2)	2.407(2)		
W(1)–Cl(1)	2.379(3)		
W(1)–Cl(2)	2.347(3)		
W(2)–Cl(3)	2.386(3)		
W(2)–Cl(4)	2.373(3)		
W(2)–P(1)	2.512(3)		
W(1)–P(2)	2.536(3)		
W(2)–P(3)	2.519(4)		
W(1)–P(4)	2.512(3)		
W(1)–H(1)	2.025(20)		
W(1)–H(2)	2.134(20)		
W(2)–H(1)	2.127(21)		
W(2)–H(2)	1.839(20)		
Bond angles			
H(1)–W(1)–H(2)	103.8(30)	H(1)–W(2)–H(2)	111.1(30)
W(1)–H(1)–W(2)	70.8(20)	W(1)–H(2)–W(2)	74.1(20)
Cl(1)–W(1)–W(2)	132.80(9)	Cl(2)–W(1)–W(2)	124.56(8)
Cl(3)–W(2)–W(1)	132.44(9)	Cl(4)–W(2)–W(1)	128.24(8)
Cl(2)–W(1)–Cl(1)	101.99(13)	Cl(4)–W(2)–Cl(3)	99.14(11)
Cl(1)–W(1)–P(2)	90.59(11)	Cl(1)–W(1)–P(4)	83.72(12)
Cl(2)–W(1)–P(2)	90.96(11)	Cl(2)–W(1)–P(4)	85.33(11)
Cl(3)–W(2)–P(1)	87.24(11)	Cl(3)–W(2)–P(3)	81.51(11)
Cl(4)–W(2)–P(1)	92.67(11)	Cl(4)–W(2)–P(3)	90.37(11)
W(1)–W(2)–P(1)	93.69(9)	W(2)–W(1)–P(2)	95.54(9)
W(1)–W(2)–P(3)	92.98(9)	W(2)–W(1)–P(4)	92.03(10)
P(1)–W(2)–P(3)	168.68(10)	P(4)–W(1)–P(2)	172.40(11)

4. Supplementary material

Crystallographic data (excluding structure factors) for the structures reported in this paper have been deposited with the Cambridge Crystallographic Data Center as supplementary publication nos. CCDC 131483 (**6**·$(THF)_2$), CCDC 1131484 (**2**·$(THF)_2$), and CCDC 131485 (**5**·$(THF)_4$). Copies of this information may be obtained free of charge from The Director, CCDC, 12 Union Road, Cambridge, CB2 1EZ, UK (Fax: +44-1223-336033; e-mail: deposit@ccdc.cam.ac.uk or www: http://www.ccdc.cam.ac.uk).

Complete tables of crystal data, positional and isotropic equivalent thermal parameters, anisotropic thermal parameters, bond distances, bond angles, and a listing of observed and calculated structure factors for the molecules of $W_2(\mu\text{-}O_2CC_6H_5)_2Br_2(\mu\text{-dppa})_2\cdot(THF)_2$ (**2**·$(THF)_2$), $W_2(\mu\text{-Cl})_2Cl_4(\mu\text{-dppa})_2\cdot(THF)_4$ (**5**·$(THF)_4$), and $W_2(\mu\text{-H})_2Cl_4(\mu\text{-dppa})_2\cdot(THF)_2$ (**6**·$(THF)_2$) are available from author J.L.E. upon request.

Acknowledgements

L.S. and J.E. would like to acknowledge the support of the National Science Foundation EPSCoR program (EHR 9108767) and the ARI Program (CHE 92-14521). E.V. and J.Z. acknowledge the support of the Office of Naval Research.

References

[1] K.M. Carlson-Day, J.L. Eglin, L.T. Smith, R.J. Staples, Inorg. Chem. 38 (1999) 2216.
[2] F.A. Cotton, J.L. Eglin, B. Hong, C.A. James, Inorg. Chem. 32 (1993) 2104.
[3] P.R. Sharp, R.R. Schrock, J. Am. Chem. Soc. 102 (1980) 1430.
[4] K.M. Carlson-Day, J.L. Eglin, C. Lin, T. Ren, E.J. Valente, J.D. Zubkowski, Inorg. Chem. 35 (1996) 4727.
[5] K.M. Carlson-Day, J.L. Eglin, E.J. Valente, J.D. Zubkowski, Inorg. Chim. Acta 244 (1996) 151.
[6] K.M. Carlson-Day, T.E. Concolino, J.L. Eglin, C. Lin, T. Ren, E.J. Valente, J.D. Zubkowski, Polyhedron 15 (1996) 4469.
[7] F.A. Cotton, W. Wang, Inorg. Chem. 23 (1984) 1604.
[8] T.E. Concolino, J.L. Eglin, J. Cluster Sci. 8 (1997) 461.
[9] P.E. Fanwick, W.S. Harwood, R.A. Walton, Inorg. Chem. 26 (1987) 242.
[10] F.A. Cotton, J.L. Eglin, B. Hong, C.A. James, J. Am. Chem. Soc. 114 (1992) 4915.
[11] T.E. Concolino, J.L. Eglin, E.J. Valente, J.D. Zubkowski, Polyhedron 16 (1997) 4137.
[12] F.A. Cotton, J.L. Eglin, C.A. James, Inorg. Chem. 32 (1993) 681.
[13] J.L. Eglin, E.J. Valente, K.R. Winfield, J.D. Zubkowski, Inorg. Chim. Acta 245 (1996) 81.
[14] P.A. Agaskar, F.A. Cotton, K.R. Dunbar, L.R. Falvello, C.J. O'Connor, Inorg. Chem. 26 (1987) 4051.
[15] H. Rothfuss, J.T. Barry, J.C. Huffman, K.G. Caulton, M.H. Chisholm, Inorg. Chem. 32 (1993) 4573.

[16] J.T. Barry, S.T. Chacon, M.H. Chisholm, V.F. DiStasi, J.C. Huffman, W.E. Streib, W.G. Van Der Sluys, Inorg. Chem. 32 (1993) 2322.
[17] F.A. Cotton, S.K. Mandal, Inorg. Chem. 31 (1992) 1267.
[18] F.A. Cotton, R.A. Walton, Multiple Bonds between Metal Atoms, 2nd edition, Oxford University Press, Oxford, 1993.
[19] D.I. Arnold, F.A. Cotton, F. Kuhn, Inorg. Chem. 35 (1996) 5764.
[20] J.M. Canich, F.A. Cotton, L.M. Daniels, D.B. Lewis, Inorg. Chem. 26 (1987) 4046.
[21] D.I. Arnold, F.A. Cotton, F.E. Kuhn, Inorg. Chem. 35 (1996) 4733.
[22] F.A. Cotton, F.E. Kuhn, Inorg. Chim. Acta 252 (1996) 257.
[23] F.A. Cotton, F.E. Kuhn, A. Yokochi, Inorg. Chim. Acta 252 (1996) 251.
[24] F.A. Cotton, J.L. Eglin, C.A. James, R.L. Luck, Inorg. Chem. 31 (1992) 5308.
[25] F.A. Cotton, T. Ren, J. Am. Chem. Soc. 114 (1992) 2237.
[26] M.D. Hopkins, H.B. Gray, V.M. Miskowski, Polyhedron 6 (1987) 705.
[27] M.D. Hopkins, W.P. Schaefer, M.J. Bronikowski, W.H. Woodruff, V.M. Miskowski, R.F. Dallinger, H.B. Gray, J. Am. Chem. Soc. 109 (1987) 408.
[28] F.A. Cotton, K.J. Wiesinger, Inorg. Chem. 31 (1992) 920.
[29] F.A. Cotton, J.L. Eglin, C.J. James, Inorg. Chem. 32 (1993) 687.
[30] R.R. Schrock, L.G. Sturgeoff, P.R. Sharp, Inorg. Chem. 22 (1983) 2801.
[31] R.S. Drago, Physical Methods for Chemists, 2nd edition, Saunders College Publishing, Ft. Worth, TX, 1992.
[32] SMARTV 4.043 Software for the CCD Detector System, Siemens Analytical Instruments Division, Madison, WI, 1996.
[33] SAINTV 4.035 Software for the CCD Detector System, Siemens Analytical Instruments Division, Madison, WI. 1995.
[34] SADABS. Program for Absorption corrections using Siemens CCD based on the method of Bob Blessing. Acta Crystallogr. A51 (1995) 33.
[35] G.M. Sheldrick, SHELXS-90, Program for the Solution of Crystal Structures, University of Gottingen, Germany, 1986.
[36] G.M. Sheldrick, SHELXL-93, Program for the Refinement of Crystal Structures, University of Gottingen, Germany, 1993.
[37] SHELXTL 5.03 (PC-Version), Program Library for Structure Solution and Molecular Graphics, Siemens Analytical Instruments Division, Madison, WI, 1995.
[38] Diffractometer data collection controlled by PE-PC version Siemens Analytical X-ray Instruments, Inc. Madison, WI.
[39] G.M. Sheldrick, Crystallographic Computing, Oxford University Press, Oxford, 1992.
[40] G.M. Sheldrick, Acta Crystallogr. A46 (1990) 467.
[41] International Tables for X-Ray Crystallography, Reidel, Dordrecht, 1985.